

Glucose-Insulin Dynamical Model for Type 2 Diabetic Patients

Mohamad Al Ahdab^a, John Leth^a, Torben Knudsen^a, Henrik Clausen^a

^aAalborg University, Denmark

Abstract

In this paper, a literature review is made for the current models of glucose-insulin dynamics of type 2 diabetes patients. Afterwards, a model is proposed by combining and modifying some of the available models in literature to take into account the effect of multiple glucose meals, multiple metformin doses, insulin injections, physical exercise, and stress on the glucose-insulin dynamics of T2D patients. The model is proposed as a candidate to be validated with real patients data in the future.

Key words: T2D, Diabetes, Glucose, Insulin, Model

1 Introduction

One of the greatest health challenges which faces humanity in the 21st century is the emergence of type 2 diabetes (T2D) as a global pandemic. More than 415 million were reported to suffer from T2D in 2015 and the number is expected to reach 642 million by 2040 [5]. Moreover, the global expenses related to T2D are estimated to be 850 million USD in 2017 and they are expected to increase [21]. T2D is characterized by high levels of glucose concentration in the blood. This increase in glucose levels can cause cardiovascular diseases and, if left untreated, will lead to organ failures. For T2D patients, low sensitivity to insulin, which is the hormone responsible for lowering glucose concentration in the blood, causes the beta cells in the pancreas to produce more of it to compensate. This will eventually weaken the cells and damage them which in turns will make the body fail to regulate glucose concentration [2]. Insulin based treatment is initiated at later stages of the T2D disease when changes in diets and physical activities accompanied with oral medications have failed. Clinically, it is difficult to calculate suitable insulin doses for each specific patient. Therefore, many patients experience uncontrolled hyperglycemia for a long period of time until they reach a safe level of glucose [28]. This happens due to the high variability of each patient and the different effect of their diet and lifestyle on insulin sensitivity. Furthermore, many patients suffer

from hypoglycemic episodes if they overdose on insulin due to inaccurate calculations. Developing a model for the glucose-insulin dynamics helps with developing and testing algorithmic insulin dose guiders that handle patients variability better and ensure a safe reach for a desired blood glucose concentration. Moreover, having a model can help in the development of hypoglycemic episodes alert systems for the patients. Additionally, models for glucose-insulin dynamics can help medical professionals with their patients' treatment plans.

In this paper, a survey of current models and simulators for the insulin-glucose dynamics in T2D patients is carried out. After that, a new model is proposed by combining and modifying some of the models from current literature. Finally, simulation results are provided to discuss the introduced model.

2 Literature Review

In general, there are two main categories of methods to model systems: first principles methods, or data driven methods derived by fitting data to general mathematical structures such as ARMAX models.

The glucose-insulin dynamical models for T2D patients based on first principles can vary with different degrees of complexity. Generally in the literature, there exist two main categories of such models: minimal models and maximal models [6]. Maximal models are very detailed models which model metabolic functions at a molecular level. On the other hand, minimal models

Email addresses: Maah@es.aau.dk (Mohamad Al Ahdab), jjl@es.aau.dk (John Leth), tk@es.aau.dk (Torben Knudsen), hgcl@es.aau.dk (Henrik Clausen).

are less detailed and rely mostly on compartments and mass balance equations. While maximal models provide a great level of accuracy, the amount of different data which is required to estimate parameters for the models is large and difficult to obtain from patients undergoing typical treatment plans. Moreover, the high accuracy of maximal models provides little relevance to the accuracy of the general glucose-insulin dynamics within the human body [6].

In contrast, minimal models consist of compartments to represent the distribution, diffusion, and production of glucose and insulin in the body with terms to represent the interaction between them. Furthermore, these models include pharmacokinetic equations to describe exogenous insulin injections and the intake of other medications. Several simulation oriented models for type 1 diabetic (T1D) patients were developed such as the ones in [19][16][14]. The models for T1D patients can be extended to model T2D patients by including dynamics for endogenous insulin production and by obtaining new probability distributions for their parameters with the use of T2D patients data. As for already existing T2D models, Cobelli's model in [7] is a detailed model for glucose-insulin dynamics which is intended for simulation use. It includes nonlinear terms with hybrid differential equations. The model parameters are mainly estimated from people who do not suffer from diabetes. However, general parameters for T2D patients were also estimated using data from T2D patients. Although the model does not consider molecular level dynamics, its level of complexity still requires a variety of measured variables to estimate parameters for a given patient. In addition to glucose measurement in the plasma, the model used traced consumed glucose data, plasma insulin concentration measurements, and data regarding C-peptides (Amino Acids molecules which are side product of insulin secretion). The authors in [7] provided only mean parameters for T2D patients. They later developed an official simulator based on an extended version of their model to account for oral medications, Glucagon, and physical activities. The simulator is reported to have joint probability distribution for the parameters of T2D patients [27]. Nevertheless, these distributions were not published. Moreover, there are no published material for the equations and the structure of the extended model. Another detailed model is recently developed by [9]. It is an extension from the model in [23]. The model includes the affect of oral medications, Glucagon, and Glucagon-like peptide-1. The model is provided with mean parameters. Some of the parameters are identified from clinical data, while others are taken from different sources of literature. None of the mentioned T2D models so far considers or provide a mathematical structure for injected insulin, ingestion of multiple meals, and physical activity. A simpler T2D simulation oriented model with insulin injection is provided in [22]. It was developed as an extension to the model

in [15] to take into account when both fast acting and long acting insulin are used for treatment. The model also uses modulator functions to account for the circadian rhythm in the glucose-insulin dynamics. As for parameter estimation, the model requires data of consumed glucose, glucose concentration in the plasma, injected insulin, and endogenous insulin concentration to be identifiable. In [22], parameter estimation was carried out using data from two different trials with different types of insulin with a total of 29 T2D patients. The parameter estimation took into account inter-individual variety by estimating a mean and a variance for the parameters. Therefore, the model can be used to simulate a population of T2D patients. The model, however, is simple and does not include oral medications, physical activity, and glucose ingestion. Another model is the one from [1]. This model requires plasma glucose measurement with injected insulin concentration data. Therefore, this model can be validated, improved, and fitted with data collected from patients during typical treatment plans as done by the work in []. The model takes the T1D model in [16] and extended it with a term to describe endogenous insulin production. The model, nevertheless, does not include a mathematical structure for physical activity or oral medications. Probability distribution for the model parameters can be found in [1].

For data driven models, several methods were attempted for T1D in [13,10,26] and T2D in [20]. These models were generally developed to predict and detect hypoglycemic risks. However, data driven models are difficult for the purpose of developing a general model for T2D patients simulations. One major problem is that when data is collected from patients, the patients are already following some form of a feedback control mechanism between measured glucose levels and injected insulin. Therefore, fitting models on data from insulin inputs to glucose output will also include the dynamics of the feedback mechanism. This is undesired when the model is intended to test different control algorithms or if it is intended for the development of control strategies. This problem can be solved by perturbing the input insulin doses with time varying functions. However, it is difficult to impose perturbation on the insulin input for the patients without affecting their comfort and health.

In this work, it is intended to provide a model with mathematical structures for the effect of multiple glucose meals, insulin injections, multiple oral doses of metformin with different sizes, physical activity, and stress. The model is based on the one in [9] with modifications and inclusions as following (see figure 1):

- Modifying the model to account for multiple meals (see section 3.1).
- Including a model for insulin injections based on [18] (see section 3.2).

- Modifying the metformin model to account for multiple different doses in section 3.3.
- Including the effect of physical activity based on [4] (see section 3.4).
- Including the effect of stress based on [11] (see section 3.5).

In addition, two simulation cases are provided in section 4 to demonstrate the effect of lifestyle changes with the model. The model proposed in this paper is intended to be used as a starting point for developing an open source simulator for T2D patients when data is available. All the simulations in the paper are done with a Matlab code which can be obtained upon request from the authors. The model parameters which are used in the simulations are found in B.1.

3 Model Description

The model is mainly based on the one from [9] with the following four main subsystems:

- Glucose subsystem.
- Insulin subsystem.
- Glucagon subsystem.
- Incretins hormone subsystem.

See figure 1 for an overview of the model. The glucose and insulin subsystems are modelled as a set of compartments representing different main parts of the human body: brain, heart and lungs, guts, liver, kidney, and peripherals. The flow between these compartments follows the human blood cycle. As for the glucagon and the incretins, a single compartment is used for each one of them as it is assumed that glucagon and incretins have equal concentration in all the body parts. In addition, the model contains metabolic production and uptake rates for different compartments. These metabolic rates are generally defined as their basal values multiplied with scaling variables that depend on the concentrations of insulin, glucose, and/or glucagon (see (A.1)). The pancreas has a different nonlinear and hybrid model. In addition, a glucose ingestion model based on [7] is included as in [25] but modified to handle multiple meals along the day. Moreover, metformin and vildagliptin oral treatment models are included based on [24] and [17] respectively as in [9] but with a modification on the oral metformin model to handle different oral doses along the treatment. Additionally, a physical activity model based on [4] is added to the model. Furthermore, long acting and fast acting insulin injection models based on [18] are added. Finally, stress is included as a factor $\alpha_s \in [0, 1]$ as in [11]. The main model includes parameters that were estimated by [23] for a healthy 70 kg male. The work in [25] considered a subset of these parameters to be estimated for the diabetic cases. Parameters for the different added models are taken from their corresponding literature. In the following

subsections, the added and modified models and states will be discussed. The full model equations are provided in appendix A.

3.1 Glucose Absorption Model

In this section, a modification is introduced to account for multiple glucose meal sizes. The model used for glucose absorption in [9] considers only one glucose meal and was used for oral glucose tests where the patient were given an oral glucose dose and asked to fast while data is collected. The model is given as:

$$\frac{dq_{S_s}}{dt} = -k_{12q}q_{S_s} \quad (1a)$$

$$\frac{dq_{S_l}}{dt} = -k_{\text{empt}}q_{S_l} + k_{12q}q_{S_s} \quad (1b)$$

$$\frac{dq_{\text{int}}}{dt} = -k_{\text{abs}}q_{\text{int}} + k_{\text{empt}}q_{S_l} \quad (1c)$$

$$k_{\text{empt}} = k_{\text{min}} + \frac{k_{\text{max}} - k_{\text{min}}}{2} \left\{ \begin{aligned} & \tanh \left[\varphi_1 (q_{S_s} + q_{S_l} - k_{\varphi_1} D_q) \right] \\ & - \tanh \left[\varphi_2 (q_{S_s} + q_{S_l} - k_{\varphi_2} D_q) \right] + 2 \end{aligned} \right\} \quad (1d)$$

$$\varphi_1 = \frac{5}{2D_q(1 - k_{\varphi_1})} \quad (1e)$$

$$\varphi_2 = \frac{5}{2D_q(k_{\varphi_2})} \quad (1f)$$

$$Ra = f_q k_{\text{abs}} q_{\text{int}} \quad (1g)$$

Where $q_{S_s}(0) = D_q$ [mg] is the oral glucose quantity, Ra is the rate of glucose appearance in the blood, f_q is an absorption factor, k_{12} [min^{-1}] and k_{abs} [min^{-1}] are the rate constants for glucose transfer to stomach and glucose absorption in the intestines respectively, k_{empt} [min^{-1}] is a rate parameter for emptying the stomach of glucose to the intestines. This parameter can have values between k_{min} and k_{max} depending on the glucose dose size D_q . In order to make the model handle different meals with different time instants, the parameter D_q needs to be modified according to the meal sizes and time. The following are the proposed modifications:

$$\frac{dq_{S_s}}{dt} = -k_{12q}q_{S_s} + \sum_{i=1}^{N_q(t)} u_{q_i} \delta(t - t_i), \quad i \in \mathbb{Z}_+ \quad (2a)$$

$$\frac{dD_e}{dt} = -k_q D_e + \sum_{i=1}^{N_q(t)} u_{q_i} \delta(t - t_i) \quad (2b)$$

$$\frac{dD_q}{dt} = k_q \left(u_{q_{N_q(t)}} - D_q \right) + D_m \sum_{i=1}^{N_q(t)} \delta(t - t_i) \quad (2c)$$

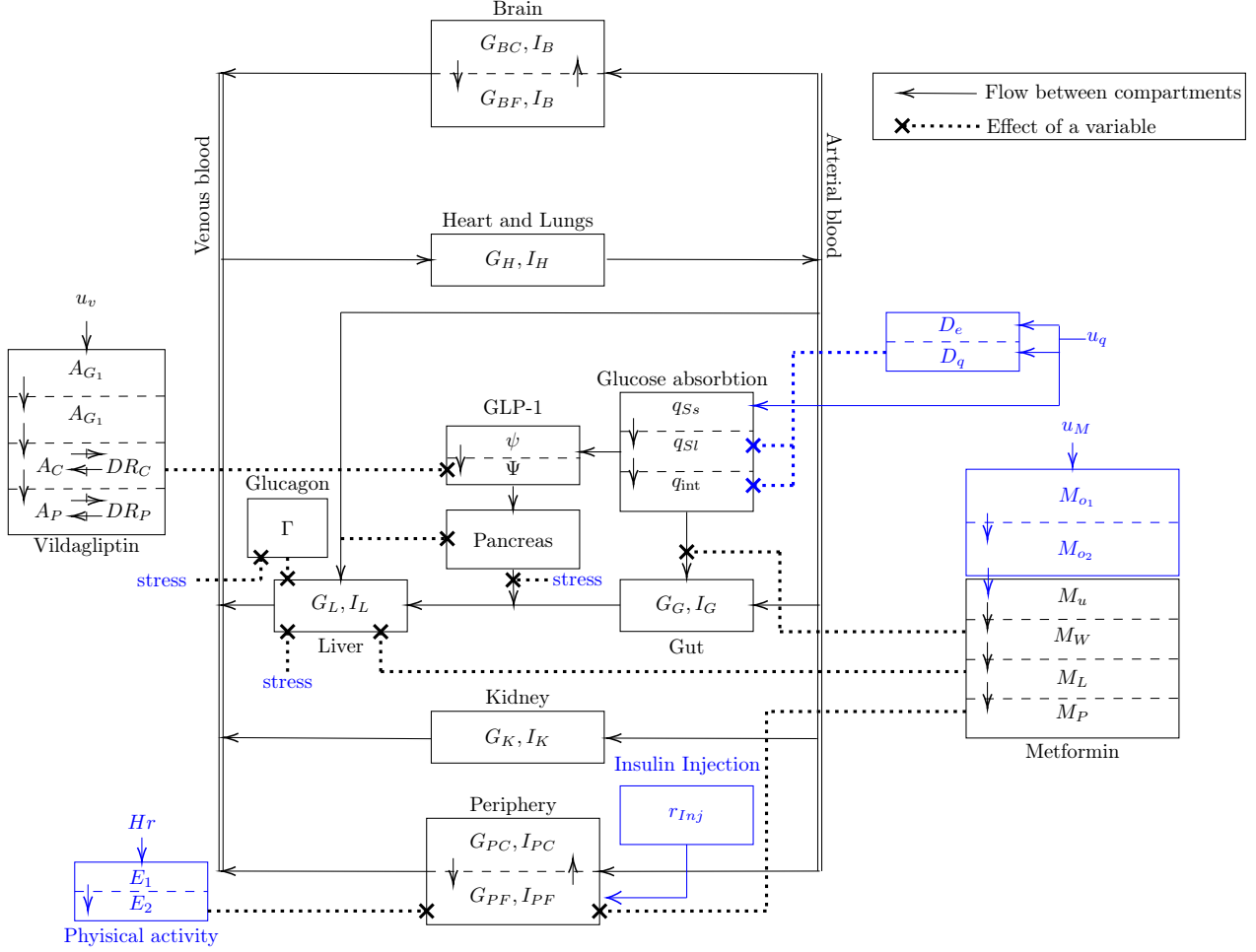


Fig. 1. A summary of the overall model with blue indicating the modified or added models compared to [9]

$$D_m = \begin{cases} D_e - D_q & u_{qN_q(0)} \neq 0 \\ 1 & u_{qN_q(0)} = 0 \end{cases} \quad (2d)$$

Where $q_{Ss}(0) = 0$, $D_e(0) = 0$, $\delta(t - t_i)$ is the Dirac delta distribution, t_i is the time instance for meal i , $N_q(t)$ is the integer number of meals until time t , u_{q_i} [mg] is the amount of oral carbohydrates intake for meal i . The state D_e is introduced to handle the accumulation of carbohydrates meals with a decay factor k_q [min^{-1}] in order to remove the effect of meals with time. With that, parameter D_q is now a state updated by D_e each time a new meal is consumed and made to converge to the last given meal amount u_{q_i} with the same rate factor k_q such that it converges to the original model through time if no meal is consumed afterwards. Note that $D_q(0) = 0$ when a zero carbohydrates meal ($u_{qN_q(0)} = 0$) is assumed at time $t = 0$, which leads to (1d) being undefined ($\varphi_1 q_{Ss} = \infty$). To avoid this, the state $D_m(0)$ is set to 1 when $u_{qN_q(0)} = 0$. Note that the value $D_m(0)$ can have any nonzero value in the case of zero carbohydrates meal at $t = 0$. The value $D_m(0)$ will not affect the rate

of glucose appearance in the plasma since the states q_{Ss} for ingested carbohydrates, and D_e for the effect of accumulation of meals depend on $u_{qN_q(0)}$ and not D_m . Parameters f_q , k_{φ_1} , and k_{φ_2} are known and taken from [7]. The rest of the parameters, k_{12q} , k_{\min} , k_{\max} , k_{abs} , and k_q are to taken to be the mean parameters which were estimated in [25]. The introduced parameter k_q has no estimate. Therefore, it is assumed to be equal to k_{\min} .

A simulation of a patient with the modified meals model compared against the unmodified one is shown in Figure 2. The patient is consuming a breakfast meal of 30 [g] carbohydrates, a second breakfast meal of 10 [g] carbohydrates, a lunch meal of 50 [g] carbohydrates, an afternoon snack of 10 [g] carbohydrates, and a dinner meal of 110 [g] carbohydrates. The simulated patient has a basal value of $G_{PC}(0) = 8$ [mmol L^{-1}] for glucose concentration in the central periphery compartment and $I_{PF} = 1$ [mUL^{-1}] for the insulin concentration in the interstitial fluid periphery compartment. It can be seen from the simulation results that the glucose appearance in plasma is distributed in a larger window of time with

lower peaks for meals that are close to each other. This is due to the reduction of the stomach emptying rate k_{empt} in response to increased accumulation of ingested carbohydrates captured by the state D_q . Additionally, glucose appearance in plasma for the modified model in response to meals after hours of fasting closely resembles the glucose appearance in plasma for the unmodified model as can be seen for the dinner and breakfast meal. This is intended since the unmodified model was proposed for fasting conditions.

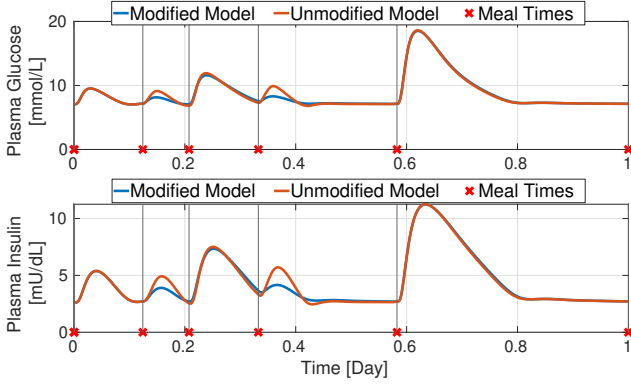


Fig. 2. Simulation results for the modified glucose absorption model against the unmodified one.

3.2 Insulin Injection Model

In this section, a model for long acting and fast acting insulin injections based on the one from [18] is introduced in [9]. Both fast and long acting insulin analogues treatments are considered for the model. When analogue insulin is injected, it dissociates from its hexameric form to dimers and monomers which then can penetrate the capillary membrane and get absorbed into the plasma. For fast acting insulin, only two compartments are considered: a compartment for insulin in its hexameric form, and a compartment for insulin in its dimeric and monomeric form. The following are the equations for fast acting insulin:

$$\frac{dH_{fa}}{dt} = \sum_{i=1}^{N_{fa}(t)} \delta(t - t_i) \frac{10}{V_{PF}^I} u_{fi} - p_{fa} \left(H_{fa}(t) - q_{fa} D_{fa}^3(t) \right) \quad (3a)$$

$$\frac{dD_{fa}}{dt} = p_{fa} \left(H_{fa}(t) - q_{fa} D_{fa}^3(t) \right) - \frac{b_{fa} D_{fa}(t)}{1 + I_{PF}(t)} \quad (3b)$$

Where H_{fa} [mU dL⁻¹] is the concentration of injected fast acting insulin in its hexameric form, D_{fa} [mU dL⁻¹] is the concentration of insulin in its dimeric and monomeric form, $N_{fa}(t)$ is the number of injected fast acting insulin doses until time t , u_{fi} [mU]

is the amount of injected fast acting insulin, b_{fa} [min⁻¹] is a constant for the infusion of fast acting insulin into the body, p_{fa} [min⁻¹] is a constant diffusion parameter, q_{fa} [dL² mU⁻²] is a constant such that $p_{fa} q_{fa}$ is the parameter for fast acting insulin dimers converting back to hexamers, and I_{PF} [mU dL⁻¹] is the insulin concentration in the interstitial periphery compartment. Parameters for Lispo and Aspart insulin injection are reported in [18]. For long acting insulin, an extra state delay in the dissociation of hexameric insulin to dimers and monomers:

$$\frac{dB_{la}}{dt} = \sum_{i=1}^{N_{la}(t)} \delta(t - t_i) \frac{10}{V_{PF}^I} u_{li} - k_{la} B_{la} \frac{C_{\max}}{1 + H_{la}} \quad (4a)$$

$$\frac{dH_{la}}{dt} = k_{la} B_{la} \frac{C_{\max}}{1 + H_{la}} - p_{la} \left(H_{la} - q_{la} D_{la}^3 \right) \quad (4b)$$

$$\frac{dD_{la}}{dt} = p_{la} \left(H_{la} - q_{la} D_{la}^3 \right) - \frac{b_{la} D_{la}}{1 + I_{PF}} \quad (4c)$$

Where B_{la} [mU dL⁻¹] is the added bound state for the concentration of hexameric insulin before diffusing, H_{la} [mU dL⁻¹] is the concentration of injected long acting insulin in its hexameric form, D_{la} [mU dL⁻¹] is the concentration of injected insulin in its dimeric and monomeric form, $N_{la}(t)$ is the number of injected long acting insulin doses until time t , u_{li} [mU] is the amount of long acting insulin dose at time t_i , b_{la} [min⁻¹] is a constant for the infusion of long acting insulin into the body, p_{la} [min⁻¹] is a constant diffusion parameter for long acting insulin, q_{la} [dL² mU⁻²] is a constant such that $p_{la} q_{la}$ is the parameter for long acting insulin dimers converting back to hexamers, k_{la} [min⁻¹] is a constant absorption rate, and C_{\max} is a dimensionless maximum transmission capacity constant. Parameters for insulin Glargin are reported in [18]. The injected insulin enters the interstitial periphery compartment (A.10g) with the following rate r_{inj} :

$$r_{inj} = V_{PF}^I \frac{r_{la} b_{la} D_{la}}{1 + I_{PF}} + V_{PF}^I \frac{r_{fa} b_{fa} D_{fa}}{1 + I_{PF}} \quad (5)$$

Where $r_{la}, r_{fa} \leq 1$ are the fractions of long acting and fast acting insulin that get to the periphery compartment, and V_{PF}^I [L] is the volume of the interstitial compartment. Figure 3 shows a simulation for a patient having the same basal values and following the same meal plan as the simulation discussed in section 3.1. The patient takes a long acting insulin dose of 50 [U] everyday an hour before the breakfast meal. Additionally, the patient takes a 30 [U] of fast acting insulin 15 minutes before dinner. Long acting insulin lower the glucose concentration over a large window of time. Moreover, the fast acting insulin helps at reducing the glucose peak after dinner.

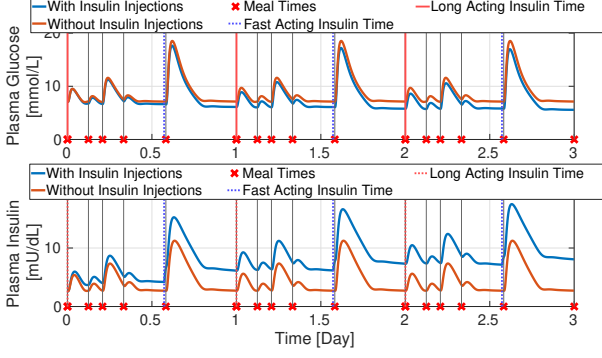


Fig. 3. A simulation showing the effect of injected insulin on glucose and insulin concentrations.

3.3 Metformin

In this section, a modification for the metformin model in [9] is carried out to account for multiple doses of oral metformin with different amounts. The metformin model used in [9], including the pharmacokinetic and its interaction with full glucose-insulin dynamical models, is based on [24]. The pharmacokinetic model of metformin in [24] is given as following:

$$\frac{dM_{GL}}{dt} = -M_{GL}(k_{go} + k_{gg}) + M_O \quad (6a)$$

$$\frac{dM_{GW}}{dt} = M_{GL}k_{gg} + M_Pk_{pg} - M_{GW}k_{gl} \quad (6b)$$

$$\frac{dM_L}{dt} = M_{GW}k_{gl} + M_Pk_{pl} - M_Lk_{lp} \quad (6c)$$

$$\frac{dM_P}{dt} = M_Lk_{lp} - M_P(k_{pl} + k_{pg} + k_{po}) + M_{GL} \quad (6d)$$

Where M_{GL} [μg] is the metformin amount in the gastrointestinal lumen, parameters $k_{go}, k_{gg}, k_{pg}, k_{gl}, k_{pl}, k_{lp}, k_{po}$ [min^{-1}] are transfer rate constants between the compartments, and M_O is the flow rate of orally ingested metformin which is modelled as:

$$M_O = Ae^{-\alpha_M t} + Be^{-\beta_M t} \quad (7)$$

Where A, B [$\mu\text{g min}^{-1}$] and α_M, β_M [min^{-1}] are constant parameters that were identified in [24]. These parameters were identified with data in which patients were taking only a 500 [mg] oral dose of metformin. Therefore, the model is modified in this work to take into account different amount of doses at different times by introducing the following:

$$\frac{dM_{O1}}{dt} = -\alpha_M M_{O1} + \sum_{i=1}^{N_M(t)} \delta(t - t_i) u_{M_i} \quad (8a)$$

$$\frac{dM_{O2}}{dt} = -\beta_M M_{O2} + \sum_{i=1}^{N_M(t)} \delta(t - t_i) u_{M_i} \quad (8b)$$

$$M_O = \rho_\alpha M_{O1} + \rho_\beta M_{O2} \quad (8c)$$

With $N_M(t)$ being the number of consumed doses of metformin until time t , u_{M_i} [μg] is the amount of metformin consumed at time t_i , and the constants $\rho_\alpha = A/(500000 [\mu\text{g}]) [\text{min}^{-1}]$ and $\rho_\beta = B/(500000 [\mu\text{g}]) [\text{min}^{-1}]$ are rate parameters. Figure 4 shows a simulation result of the same patient in section 3.1 taking metformin doses of 500 [mg] for the first two days and then a metformin dose of 1000 [mg] for the last two days. The 1000 [mg] dose prolong the effect of metformin on lowering the glucose concentration when compared to the dose of 500 [mg].

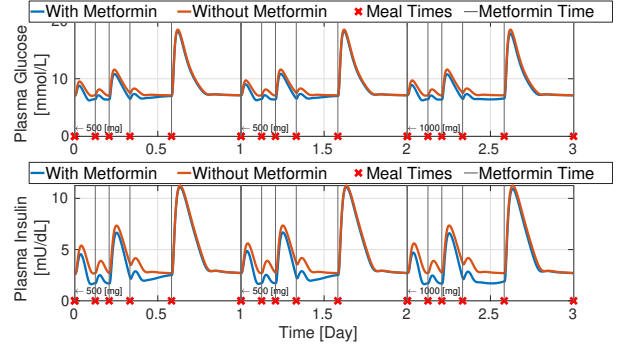


Fig. 4. A simulation showing the effect of metformin on glucose and insulin concentrations.

3.4 Physical Activity Model

In this section, a physical activity model based on [4] is added to the model in [9]. The model in [4] was developed for a T1D model based on [3]. The model considers the change of the heart beat following a physical activity to be the stimulus of two states E_1 and E_2 which are dimensionless:

$$\frac{dE_1}{dt} = -\frac{1}{\tau_{HR}} E_1 + \frac{1}{\tau_{HR}} (\text{HR} - \text{HR}_b) \quad (9a)$$

$$\frac{dE_2}{dt} = -\left(g_e(E_1) + \frac{1}{\tau_e}\right) E_2 + g_e(E_1) \quad (9b)$$

$$g(E_1) = \frac{\left(\frac{E_1}{a_e \text{HR}_b}\right)^{n_e}}{1 + \left(\frac{E_1}{a_e \text{HR}_b}\right)^{n_e}} \quad (9c)$$

Where t_{HR}, τ_e [min] are time constants, HR, HR_b [bpm] are the current and rest heart rates respectively, and the parameters a_e, n_e are dimensionless parameters. The first state E_1 is used directly as a stimulus to increase the insulin-independent glucose uptake in response to a physical activity while the state E_2 is used for the longer lasting change of insulin action on glucose. The glucose and insulin model structure in [4] is simpler than the one considered in this work. Nevertheless, the inclusion of the physical activity for the model in this

work is similar to how other models include physical activity, e.g., see [8]. With that, the effect of the state E_1 is included as an increase in the clearance rate of glucose in the periphery interstitial fluid compartment with a constant parameter β_e [bpm $^{-1}$] as $\frac{1}{T_P} (1 + \beta_e E_1)$ where $\frac{1}{T_P}$ [min $^{-1}$] is the clearance rate for glucose in the periphery interstitial fluid compartment in (A.3h). The effect of E_1 can be removed to obtain the original model by setting $\beta_e = 0$. As for the effect on insulin action, the state E_2 is introduced on the glucose metabolic rates which depend on insulin as following:

- An increase in the periphery glucose uptake rate r_{PGU} in the the interstitial fluid periphery compartment (A.3h) by a constant α_e as $(1 + \alpha_e E_2) r_{PGU}$.
- An increase in the hepatic glucose uptake rate r_{HGU} in the liver compartment (A.3e) with a constant α_e as $(1 + \alpha_e E_2) r_{HGU}$.
- A decrease in the hepatic glucose production rate r_{PGH} in the liver compartment (A.3e) with a constant α_e as $(1 + \alpha_e E_2) r_{HGP}$.

The effect of E_2 can be removed to obtain the original model by setting $\alpha_e = 0$. The parameters for the physical activity model are taken from [4] except for α_e and β_e which were tuned to have a similar effect to the ones demonstrated in [4,8]. Figure 5 shows a simulation for the patient described in section 3.1 when the patient exercise everyday before dinner raising the heart rate from a rest value of 80 [bpm] to a value of 140 [bpm] for 30 minutes. The immediate effect of physical activity is seen in the simulation results. In addition, the prolonged effect of physical activity on insulin action on glucose is seen in the figure.

3.5 Stress Effect

In this section, the effect of stress is included in the model [9]. In [11], the effect of stress was included as a multiplicative factor $1 + \alpha_s$, with $\alpha_s \in [0, 1]$, to the glucose and glucagon production rates. This is based

on the fact that stress causes a direct increase in the pancreatic glucagon production through an increase in catecholamines which in turns drives an increase of glucose production in the liver [29]. In addition, stress was also included as a multiplicative factor $1 - \alpha_s$ to the pancreatic insulin secretion rate based on [29]. Similarly in this work, the effect of stress is included in the model as following:

- An increase in the plasma glucagon release rate r_{PGR} in the glucagon compartment (A.9a) as $(1 + \alpha_s) r_{PGR}$.
- An increase in the hepatic glucose production rate r_{HGP} in the glucose liver compartment (A.3e) as $(1 + \alpha_s) r_{HGP}$.
- A decrease in the pancreatic insulin release rate r_{PIR} in the insulin liver compartment (A.10d) as $(1 - \alpha_s) r_{PIR}$.

Figure 6 shows the effect of stress in a simulation for the same patient discussed in section 3.1 when the patient is stressed on the second day with α_s ramping up from 0 to 0.4 in 6 hours, staying at 0.4 for 12 hours, and then ramping down to 0 for the rest of the day. Stress manages to increase glucose concentration together with a decrease in insulin concentration.

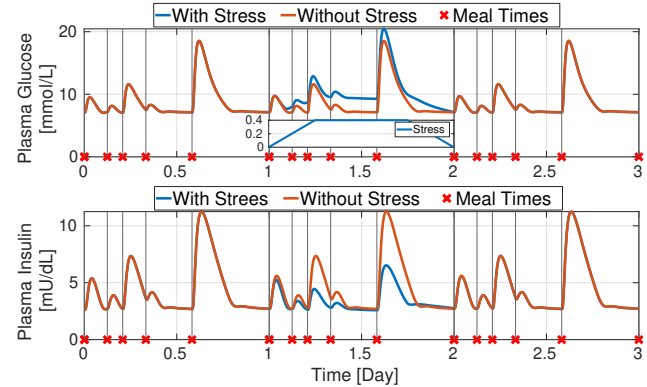


Fig. 6. A simulation showing the effect of stress on glucose and insulin concentrations.

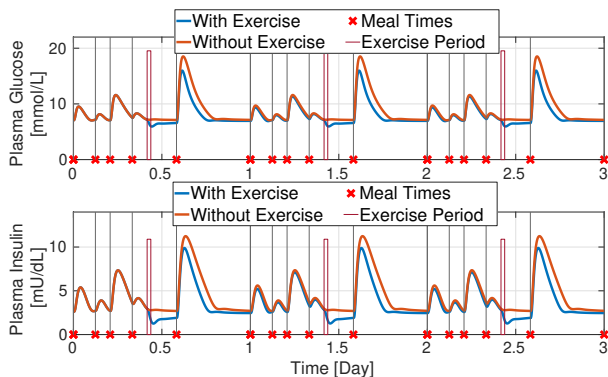


Fig. 5. A simulation showing the effect of physical activity on glucose and insulin concentrations.

4 Simulation Results

In this section, two simulation cases are carried out and discussed briefly to show how the model incorporates the effect of lifestyle changes on type 2 diabetic patients. The first case is for a patient having the same basal values and meal plan as the one discussed in section 3.1. Additionally, the patient experiences stress on the second day in the same manner as for the patient discussed in section 3.5. Moreover, the patient takes a 1000 [mg] oral dose of metformin together with long acting insulin dose of 50 [U] everyday an hour before breakfast. Furthermore, the patient take a fast acting insulin dose of 30 [U] 15 minutes before dinner. Figure

7 shows the results of the simulation for this case. The patient manages to reach a fasting plasma glucose concentration of 6 [mmolL⁻¹] towards the end of the third day.

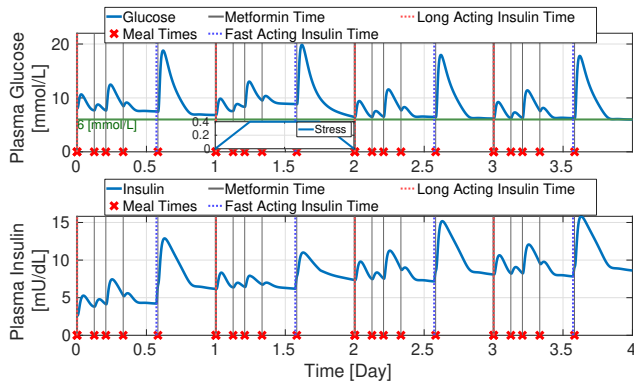


Fig. 7. Simulation results for a the first case patient.

For the second simulation case, the patient has the same basal values and meal plan as the first case patient. However, the patient does not experience stress and perform moderate exercise everyday raising the heart rate from 80 [bpm] to 120 [bpm] for a period of 30 minutes four hours before dinner. Additionally, the patient only takes a long acting insulin dose of 30 [U] and an oral metformin dose of 500 [mg] an hour before breakfast. Figure 8 shows the second case simulation results. While the patient does not achieve a fasting

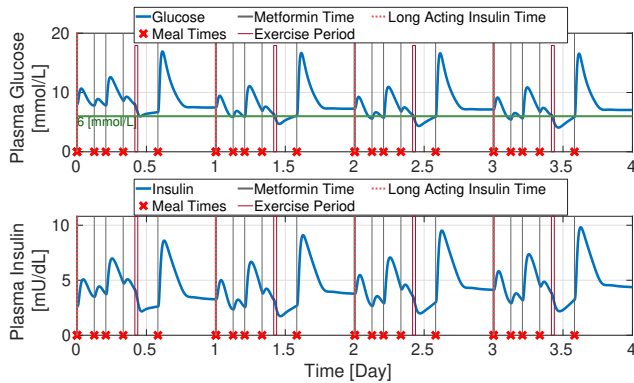


Fig. 8. Simulation results for a the second case patient.

plasma glucose concentration of 6 [mmolL⁻¹] by the end of the third day, the patient in the second case has lower plasma glucose concentrations during the day when compared to the first patient.

5 Conclusion and Future Work

The proposed model is shown to be able to be used with multiple glucose meal sizes, different metformin doses, physical activity, insuling injections, and stress. The model, however, need to be confirmed with real patients

data. Moreover, real patient data can be used to estimate joint probability distribution to model a population of T2D patients.

References

- [1] Tinna B. Aradóttir, Dimitri Boiroux, Henrik Bengtsson, Jonas Kildegaard, Brad V. Orden, and John B. Jørgensen. Model for simulating fasting glucose in type 2 diabetes and the effect of adherence to treatment. *IFAC-PapersOnLine*, 50(1):15086 – 15091, 2017. 20th IFAC World Congress.
- [2] Sabine Arnolds, Tim Heise, Frank Flacke, and Jochen Sieber. Common standards of basal insulin titration in T2DM. *Journal of Diabetes Science and Technology*, 7(3):771–788, 2013. PMID: 23759411.
- [3] Richard N Bergman, Y Ziya Ider, Charles R Bowden, and Claudio Cobelli. Quantitative estimation of insulin sensitivity. *American Journal of Physiology-Endocrinology And Metabolism*, 236(6):E667, 1979.
- [4] Marc D Breton. Physical activity—the major unaccounted impediment to closed loop control, 2008.
- [5] N.H. Cho, J.E. Shaw, S. Karuranga, Y. Huang, J.D. da Rocha Fernandes, A.W. Ohlrogge, and B. Malanda. Id diabetes atlas: Global estimates of diabetes prevalence for 2017 and projections for 2045. *Diabetes Research and Clinical Practice*, 138:271 – 281, 2018.
- [6] Claudio Cobelli, Chiara Dalla Man, Giovanni Sparacino, Lalo Magni, Giuseppe De Nicolao, and Boris P Kovatchev. Diabetes: models, signals, and control. *IEEE reviews in biomedical engineering*, 2:54–96, 2009.
- [7] C. Dalla Man, R. A. Rizza, and C. Cobelli. Meal simulation model of the glucose-insulin system. *IEEE Transactions on Biomedical Engineering*, 54(10):1740–1749, Oct 2007.
- [8] Chiara Dalla Man, Marc D Breton, and Claudio Cobelli. Physical activity into the meal glucose—insulin model of type 1 diabetes: In silico studies, 2009.
- [9] Marziyeh Eftekhari and Omid Vahidi. Mechanism based pharmacokinetic pharmacodynamic modeling of vildagliptin as an add-on to metformin for subjects with type 2 diabetes. *Computer Modeling in Engineering & Sciences*, 114(2):153–171, 2018.
- [10] Mirela Frandes, Bogdan Timar, Romulus Timar, and Diana Lungeanu. Chaotic time series prediction for glucose dynamics in type 1 diabetes mellitus using regime-switching models. *Scientific reports*, 7(1):6232, 2017.
- [11] Lu Gaohua and Hidenori Kimura. A mathematical model of brain glucose homeostasis. *Theoretical biology and medical modelling*, 6(26), 2009.
- [12] Alan J Garber. Incretin therapy—present and future. *The review of diabetic studies: RDS*, 8(3):307, 2011.
- [13] Eleni I. Georga, Vasilios C. Protopappas, and Dimitrios I. Fotiadis. Glucose prediction in type 1 and type 2 diabetic patients using data driven techniques. In Kimito Funatsu, editor, *Knowledge-Oriented Applications in Data Mining*, chapter 17. IntechOpen, Rijeka, 2011.
- [14] Roman Hovorka, Valentina Canonico, Ludovic J Chassin, Ulrich Haueter, Massimo Massi-Benedetti, Marco Orsini Federici, Thomas R Pieber, Helga C Schaller, Lukas Schaupp, Thomas Vering, and Malgorzata E Wilinska. Nonlinear model predictive control of glucose concentration in subjects with type 1 diabetes. *Physiological Measurement*, 25(4):905–920, jul 2004.

[15] Petra M. Jauslin, Nicolas Frey, and Mats O. Karlsson. Modeling of 24-hour glucose and insulin profiles of patients with type 2 diabetes. *The Journal of Clinical Pharmacology*, 51(2):153–164, 2011.

[16] Sami S. Kanderian, Stu Weinzimer, Gayane Voskanyan, and Garry M. Steil. Identification of intraday metabolic profiles during closed-loop glucose control in individuals with type 1 diabetes. *Journal of Diabetes Science and Technology*, 3(5):1047–1057, 2009. PMID: 20144418.

[17] Cornelia B Landersdorfer, Yan-Ling He, and William J Jusko. Mechanism-based population modelling of the effects of vildagliptin on glp-1, glucose and insulin in patients with type 2 diabetes. *British journal of clinical pharmacology*, 73(3):373–390, 2012.

[18] Jiaxu Li and James D Johnson. Mathematical models of subcutaneous injection of insulin analogues: a mini-review. *Discrete and continuous dynamical systems. Series B*, 12(2):401, 2009.

[19] Chiara Dalla Man, Francesco Micheletto, Dayu Lv, Marc Breton, Boris Kovatchev, and Claudio Cobelli. The uva/padova type 1 diabetes simulator: New features. *Journal of Diabetes Science and Technology*, 8(1):26–34, 2014. PMID: 24876534.

[20] Barbara Martinovic, John Leth, Torben Knudsen, Tinna Björk Aradóttir, and Henrik Bengtsson. Modelling the glucose-insulin system of type 2 diabetes patients using armax models. In *2019 Australian & New Zealand Control Conference (ANZCC)*, pages 88–93. IEEE, 2019.

[21] K. Ogurtsova, J.D. da Rocha Fernandes, Y. Huang, U. Linnenkamp, L. Guariguata, N.H. Cho, D. Cavan, J.E. Shaw, and L.E. Makaroff. Idf diabetes atlas: Global estimates for the prevalence of diabetes for 2015 and 2040. *Diabetes Research and Clinical Practice*, 128:40 – 50, 2017.

[22] Rikke M. Røge, Søren Klim, Niels R. Kristensen, Steen H. Ingwersen, and Maria C. Kjellsson. Modeling of 24-hour glucose and insulin profiles in patients with type 2 diabetes mellitus treated with biphasic insulin aspart. *The Journal of Clinical Pharmacology*, 54(7):809–817, 7 2014.

[23] John Thomas Sorensen. *A physiologic model of glucose metabolism in man and its use to design and assess improved insulin therapies for diabetes*. PhD thesis, Massachusetts Institute of Technology, 1985.

[24] Lin Sun, Ezra Kwok, Bhushan Gopaluni, and Omid Vahidi. Pharmacokinetic-pharmacodynamic modeling of metformin for the treatment of type ii diabetes mellitus. *The open biomedical engineering journal*, 5:1, 2011.

[25] O Vahidi, KE Kwok, R Bhushan Gopaluni, and FK Knop. A comprehensive compartmental model of blood glucose regulation for healthy and type 2 diabetic subjects. *Medical & biological engineering & computing*, 54(9):1383–1398, 2016.

[26] John Joseph Valletta, Andrew J Chipperfield, and Christopher D Byrne. Gaussian process modelling of blood glucose response to free-living physical activity data in people with type 1 diabetes. In *2009 Annual International Conference of the IEEE Engineering in Medicine and Biology Society*, pages 4913–4916. IEEE, 2009.

[27] Roberto Visentin, Enrique Campos-Náñez, Michele Schiavon, Dayu Lv, Martina Vettoretti, Marc Breton, Boris P Kovatchev, Chiara Dalla Man, and Claudio Cobelli. The uva/padova type 1 diabetes simulator goes from single meal to single day. *Journal of diabetes science and technology*, 12(2):273–281, 2018.

[28] Kalina Wong, Diana Glovac, Shaista Malik, Stanley S. Franklin, Gail Wygant, Uchenna Iloeje, Hongjun Kan, and

Nathan D. Wong. Comparison of demographic factors and cardiovascular risk factor control among u.s. adults with type 2 diabetes by insulin treatment classification. *Journal of Diabetes and its Complications*, 26(3):169 – 174, 2012.

[29] SC Woods, D Porte Jr, E Bobbioni, E Ionescu, JF Sauter, F Rohner-Jeanrenaud, and B Jeanrenaud. Insulin: its relationship to the central nervous system and to the control of food intake and body weight. *The American journal of clinical nutrition*, 42(5):1063–1071, 1985.

A Full Model Equations

The compartments include metabolic production rates r_{CXP} and metabolic uptake rates r_{CXU} for substance X in compartment C generally defined as following:

$$r_{CXP,U} = M^I M^G M^\Gamma r_{CXP,U}^b \quad (\text{A.1})$$

Where M^I, M^G , and M^Γ are multiplicative quantities for the effect of insulin I , glucose G , and glucagon Γ respectively, and $r_{CXP,U}^b$ is the basal metabolic rate of substance X in compartment C . The general form for the multiplicative quantities representing the effect of a substance Y in compartment C with concentration Y_C is given as:

$$M^Y = \frac{a + b \tanh \left[c \left(Y_C / Y_C^b - d \right) \right]}{a + b \tanh [c(1 - d)]} \quad (\text{A.2})$$

Where Y_C^b is the basal concentration of substance Y in compartment C , and a, b, c , and d are model parameters.

A.1 Glucose Sub-Model

Applying mass balance equations over the compartments for glucose, the following equations are obtained:

$$V_{BC}^G \frac{dG_{BC}}{dt} = Q_B^G (G_H - G_{BC}) - \frac{V_{BF}^G}{T_B^G} (G_{BC} - G_{BF}) \quad (\text{A.3a})$$

$$V_{BF}^G \frac{dG_{BF}}{dt} = \frac{V_{BF}^G}{T_B^G} (G_{BC} - G_{BF}) - r_{BGU} \quad (\text{A.3b})$$

$$V_H^G \frac{dG_H}{dt} = Q_B^G G_{BC} + Q_L^G G_L + Q_K^G G_K + Q_P^G G_{PC} + Q_H^G G_H - r_{RBCU} \quad (\text{A.3c})$$

$$V_G^G \frac{dG_G}{dt} = Q_G^G (G_H - G_G) - r_{GCU}^m + Ra \quad (\text{A.3d})$$

$$V_L^G \frac{dG_L}{dt} = Q_A^G G_H + Q_G^G G_G - Q_L^G G_L + ((1 + \alpha_s)(1 - \alpha_e E_2) r_{HGP}^m - (1 + \alpha_e E_2) r_{HGU}) \quad (\text{A.3e})$$

$$V_K^G \frac{dG_K}{dt} = Q_K^G (G_H - G_K) - r_{KGE} \quad (\text{A.3f})$$

$$V_{PC}^G \frac{dG_{PC}}{dt} = Q_P^G (G_H - G_{PC}) - \frac{V_{PF}^G}{T_P^G} (G_{PC} - G_{PF}) \quad (\text{A.3g})$$

$$V_{PF}^G \frac{dG_{PF}}{dt} = \frac{V_{PF}^G}{T_P^G} (G_{PC} - (1 + \beta_e E_1) G_{PF}) - (1 + \alpha_e E_2) r_{PGU}^m \quad (\text{A.3h})$$

Where G_i [mg dL⁻¹] is glucose concentration for each compartment i , Q_i^G [dL min⁻¹] is the vascular blood flow for the glucose compartment i , V_i^G [dL] is the volume of compartment i , T_i^G [min] is the transcapillary diffusion time for compartment i , and r_{xP}, r_{xU} are metabolic glucose production and uptake rates respectively. The following are the meanings of each subscript in the model:

- B: Brain
- BC: Brain capillary space
- BF: Brain interstitial fluid
- H: Hear
- G: Guts
- L: Liver
- K: Kidney
- P: Periphery
- PC: Periphery capillary space
- PF: Periphery interstitial fluid
- BGU: Brain glucose uptake
- RBCU: Red blood cell glucose uptake
- GGU: Gut glucose uptake
- HGP: Hepatic glucose production
- HGU: Hepatic glucose uptake
- KGE: Kidney glucose excretion
- PGU: Peripheral glucose uptake

The metabolic rates for the glucose subsystem are given as:

$$r_{PGU} = M_{PGU}^I M_{PGU}^G r_{PGU}^b, r_{PGU}^b = 35 \quad (\text{A.4a})$$

$$r_{HGP} = M_{HGP}^I M_{HGP}^G M_{HGP}^\Gamma r_{HGP}^b, r_{HGP}^b = 35 \quad (\text{A.4b})$$

$$r_{HGU} = M_{HGU}^I M_{HGU}^G r_{HGU}^b, r_{HGU}^b = 20 \quad (\text{A.4c})$$

$$r_{KGE} = \begin{cases} 71 + 71 \tanh [0.11 (G_K - 460)] & G_K < 460 \\ -330 + 0.872 G_K & G_K \geq 460 \end{cases} \quad (\text{A.4d})$$

$$r_{BGU} = 70, r_{RBCU} = 10, r_{GGU} = 20 \quad (\text{A.4e})$$

Where:

$$M_{PGU}^I = \frac{7.03 + 6.52 \tanh [c_1 (I_{PF}/I_{PF}^B - d_1)]}{7.03 + 6.52 \tanh [c_1 (1 - d_1)]} \quad (\text{A.5a})$$

$$M_{PGU}^G = G_{PF}/G_{PF}^b \quad (\text{A.5b})$$

$$\frac{d}{dt} M_{HGP}^I = 0.04 (M_{HGP}^{I\infty} - M_{HGP}^I) \quad (\text{A.5c})$$

$$M_{HGP}^{I\infty} = \frac{1.21 - 1.14 \tanh [c_2 (I_L/I_L^B - d_2)]}{1.21 - 1.14 \tanh [c_2 (1 - d_2)]} \quad (\text{A.5d})$$

$$M_{HGP}^G = \frac{1.42 - 1.41 \tanh [c_3 (G_L/G_L^B - d_3)]}{1.42 - 1.41 \tanh [c_3 (1 - d_3)]} \quad (\text{A.5e})$$

$$M_{HGP}^\Gamma = 2.7 \tanh [0.39 \Gamma/\Gamma^B] - f \quad (\text{A.5f})$$

$$\frac{d}{dt} f = 0.0154 \left[\left(\frac{2.7 \tanh [0.39 \Gamma/\Gamma^B] - 1}{2} \right) - f \right] \quad (\text{A.5g})$$

$$\frac{d}{dt} M_{HGU}^I = 0.04 (M_{HGU}^{I\infty} - M_{HGU}^I) \quad (\text{A.5h})$$

$$M_{HGU}^{I\infty} = \frac{2.0 \tanh [c_4 (I_L/I_L^B - d_4)]}{2.0 \tanh [c_4 (1 - d_4)]} \quad (\text{A.5i})$$

$$M_{HGU}^G = \frac{5.66 + 5.66 \tanh [c_5 (G_L/G_L^B - d_5)]}{5.66 + 5.66 \tanh [c_5 (1 - d_5)]} \quad (\text{A.5j})$$

Note that some of these rates have a constant numerical value. In addition, parameters a and b for the multiplicative quantities are substituted with numerical values. These numerical values are the ones estimated for a healthy 70 kg male. Parameters c and d were left for the estimation in case of a diabetic patient as in [25]. The following rates are modified with the effect of metformin as following:

$$r_{GGU}^m = (1 + E_{GW}) r_{GGU} \quad (\text{A.6a})$$

$$r_{HGP}^m = (1 - E_L) r_{HGP} \quad (\text{A.6b})$$

$$r_{PGU}^m = (1 + E_P) r_{PGU} \quad (\text{A.6c})$$

Where E_{GW} , E_L , and E_P are positives coefficients which depend on the amount of metformin in the gastrointestinal wall (GI) M_{GW} [μg], liver M_L [μg], and peripherals M_P [μg] respectively. These coefficients increase (or decrease) the glucose uptake (or production) as seen in (A.6). The equations for these coefficients are given as following:

$$E_{GW} = \frac{\nu_{GW,\max} \times (M_{GW})^{n_{GW}}}{(\varphi_{GW,50})^{n_{GW}} + (M_{GW})^{n_{GW}}} \quad (\text{A.7a})$$

$$E_L = \frac{\nu_{L,\max} \times (M_L)^{n_L}}{(\varphi_{L,50})^{n_L} + (M_L)^{n_L}} \quad (\text{A.7b})$$

$$E_P = \frac{\nu_{P,\max} \times (M_P)^{n_P}}{(\varphi_{P,50})^{n_P} + (M_P)^{n_P}} \quad (\text{A.7c})$$

Where $\nu_{GW,\max}$, $\nu_{L,\max}$, $\nu_{P,\max}$ are parameters to represent the maximum effect of metformin in each one of its corresponding compartments, $\varphi_{GW,50}$, $\varphi_{L,50}$, $\varphi_{P,50}$ [μg] are the masses of metformin within the different compartments to produce half of its maximum effect, and n_{GW} , n_L , and n_P are shape factors.

A.2 Incretins Sub-Model

The incretins hormones are metabolic hormones released after eating a meal to stimulate a decrease in blood glucose levels. For T2D patients, Glucagon-Like-Peptide-1 (GLP-1) is the most active incretin [12]. GLP-1 is then modelled with the following two compartments as in [9]:

$$\frac{d\psi}{dt} = \zeta k_{\text{empt}} q_{SI} - \frac{1}{\tau_\psi} \psi \quad (\text{A.8a})$$

$$V^\Psi \frac{d\Psi}{dt} = \frac{1}{\tau_\psi} \psi - [K_{\text{out}} + (R_{\text{max}C} - DR_c) Cf_2] \Psi \quad (\text{A.8b})$$

Where τ_ψ [min^{-1}] is a time constant for the release and absorption of GLP-1 to the blood stream upon consuming a meal, V^Ψ [dL] is the volume of the GLP-1 compartment, DR_c [nmol] is the amount of Dipeptidyl peptidase-4 (DPP-4) in the central compartment deactivated by the drug vildagliptin, K_{out} [min^{-1}] is a clearance constant for GLP-1 independently of the amount of DPP-4, and $(R_{\text{max}C} - DR_c)$ is the amount of available activated DPP-4 in the blood plasma with $R_{\text{max}C}$ [nmol] being the maximum amount of active DPP-4 in the absence of the vildagliptin. Cf_2 [$\text{min}^{-1} \text{nmol}^{-1}$] is a proportionality factor for the elimination of GLP-1 by active DPP-4 [17]. Parameters τ_ψ and ζ are estimated in [25] when other incretins than GLP-1 are considered and later modified in [25] to account for vildagliptin treatment. Parameters K_{out} , $R_{\text{max}C}$, and Cf_2 were estimated in [17] together with the parameters for the vildagliptin model described in subsection A.6.

A.3 Glucagon Sub-Model

The glucagon subsystem consists of one compartment as it is assumed to have the same concentration over all the body:

$$V^\Gamma \frac{d\Gamma}{dt} = (1 + \alpha_s) r_{PGR} - 9.1\Gamma \quad (\text{A.9a})$$

$$r_{PGR} = M_{PGR}^G M_{PGR}^I r_{PGR}^b, \quad r_{PGR}^b = 9.1 \quad (\text{A.9b})$$

$$M_{PGR}^G = 1.31 - 0.61 \tanh \left[1.06 \left(\frac{G_H}{G_H^B} - 0.47 \right) \right] \quad (\text{A.9c})$$

$$M_{PGR}^I = 2.93 - 2.09 \tanh \left[4.18 \left(\frac{I_H}{I_H^B} - 0.62 \right) \right] \quad (\text{A.9d})$$

Where r_{PGR} is the plasma glucagon release rate. The state Γ represent a normalized glucagon state with respect to its basal value. This is done since it is difficult

in practice to obtain glucagon measurements for each subject in order to initialize the state. Therefore for this model, the basal glucagon state is 1.

A.4 Insulin Sub-Model

Applying mass balance equations over the insulin compartments will yield the following:

$$V_B^I \frac{dI_B}{dt} = Q_B^I (I_H - I_B) \quad (\text{A.10a})$$

$$V_H^I \frac{dI_H}{dt} = Q_B^I I_B + Q_L^I I_L + Q_K^I I_K + Q_P^I I_{PV} - Q_H^I I_H \quad (\text{A.10b})$$

$$V_G^I \frac{dI_G}{dt} = Q_G^I (I_H - I_G) \quad (\text{A.10c})$$

$$V_L^I \frac{dI_L}{dt} = Q_A^I I_H + Q_G^I I_G - Q_L^I I_L + (1 - \alpha_s) r_{PIR} - r_{LIC} \quad (\text{A.10d})$$

$$V_K^I \frac{dI_K}{dt} = Q_K^I (I_H - I_K) - r_{KIC} \quad (\text{A.10e})$$

$$V_{PC}^I \frac{dI_{PC}}{dt} = Q_P^I (I_H - I_{PC}) - \frac{V_{PF}^I}{T_P^I} (I_{PC} - I_{PF}) \quad (\text{A.10f})$$

$$V_{PF}^I \frac{dI_{PF}}{dt} = \frac{V_{PF}^I}{T_P^I} (I_{PC} - I_{PF}) - r_{PIC} + r_{inj} \quad (\text{A.10g})$$

Where r_{LIC} , r_{KIC} , and r_{PIC} are the liver, kidney, and peripherals insulin clearance rates respectively and are defined as following:

$$r_{LIC} = 0.4 \left[Q_A^I I_H + Q_G^I I_G - Q_L^I I_L + r_{PIR} \right] \quad (\text{A.11a})$$

$$r_{KIC} = 0.3 Q_K^I I_K \quad (\text{A.11b})$$

$$r_{PIC} = \frac{I_{PF}}{\left[\left(\frac{1-0.15}{0.15 Q_P^I} \right) - \frac{20}{V_{PF}^I} \right]} \quad (\text{A.11c})$$

the pancreas insulin release is calculated by the following:

$$r_{PIR} = \frac{S}{S^b} r_{PIR}^b \quad (\text{A.12})$$

Where S [U min^{-1}] is the pancreas secreted insulin rate, and S^b , r_{PIR}^b are the basal values. The model for S and S^b is described in subsection A.5.

A.5 Pancreas Sub-Model

The model consists of two main compartments: a large insulin storage compartment m_s [μg] and a small labile insulin compartment m_l [μg]. The flow of insulin from the storage compartment to the labile insulin compartment is dependent on a dimensionless

factor P with a proportionality constant γ [$\mu\text{g min}^{-1}$]. The factor P depends on a dimensionless glucose-enhanced excitation factor represented by X and GLP-1 through a linear compartment with constant first order rate α [min^{-1}]. Upon a glucose stimulus, the glucose-enhanced excitation factor X will increase instantaneously depending on the glucose increase in the plasma G_H . In addition, a dimensionless inhibitor R for X will increase in response to X through a linear compartment with a first order constant rate β [min^{-1}]. During that increase, the secreted insulin S will depend directly on both X and its inhibitor R together with GLP-1. Afterwards when R reaches X or X starts decreasing after R reaching it, the insulin secretion rate will only depend on X and GLP-1. The following are the equations of the model:

$$\frac{dm_s}{dt} = K_l m_l - K_s m_s - \gamma P \quad (\text{A.13a})$$

$$\frac{dm_l}{dt} = K_s m_s - K_l m_l + \gamma P - S \quad (\text{A.13b})$$

$$\frac{dP}{dt} = \alpha(P_\infty - P) \quad (\text{A.13c})$$

$$\frac{dR}{dt} = \beta(X - R) \quad (\text{A.13d})$$

$$S = \begin{cases} [N_1 P_\infty + N_2 (X - R) + \zeta_2 \Psi] m_l & X > R \\ (N_1 P_\infty + \zeta_2 \Psi) m_l & X \leq R \end{cases} \quad (\text{A.13e})$$

$$P_\infty = X^{1.11} + \zeta_1 \Psi \quad (\text{A.13f})$$

$$X = \frac{G_H^{3.27}}{132^{3.27} + 5.93 G_H^{3.02}} \quad (\text{A.13g})$$

Where K_l [min^{-1}] and K_s [min^{-1}] are the rates for the flow between the labile and storage insulin compartments independently of P , N_1 [min^{-1}] and N_2 [min^{-1}] are constant parameters that represent the effect of P and $(X - R)$ on the insulin secretion rate respectively, and ζ_1 [L pmol^{-1}], ζ_2 [L (pmol min)^{-1}] are constant parameters to represent the effect of GLP-1 on P_∞ and the insulin secretion rate. For initializing the model and calculating the basal values, the storage compartment is assumed to be large enough for it to be constant. Therefore, writing the mass balance for the storage compartment at zero glucose concentration will yield the following:

$$K_s m_s = K_l m_{l_0} \quad (\text{A.14})$$

Where m_{l_0} is the labile insulin concentration at zero glucose concentration. This parameter in [23] is provided with a value of 6.33 [U] for a healthy 70 kg male.

A.6 Vildagliptin

The vildagliptin model is based on [17]. The absorption of orally ingested vildagliptin is modelled by two

compartments as following:

$$\frac{dA_{G1}}{dt} = -k_{a1} A_{G1} + \sum_{i=1}^{N_v(t)} \delta(t - t_i) f_v u_{v_i} \quad (\text{A.15a})$$

$$\frac{dA_{G2}}{dt} = k_{a1} \times A_{G1} - k_{a2} \times A_{G2} \quad (\text{A.15b})$$

Where A_{G1} , A_{G2} [nmol] are the amount of vildagliptin in the gut and absorption compartments respectively, $N_v(t)$ is the number of oral vildagliptin doses until time t , u_{v_i} [nmol] is the amount of consumed vildagliptin, f_a is the bioavailability of vildagliptin, and k_{a1} , k_{a2} [min^{-1}] are rate absorption parameters. After that, the model contains a central and a peripheral compartment for the vildagliptin and the vildagliptin-DPP-4 complex (deactivated DPP-4):

$$\begin{aligned} \frac{dA_c}{dt} = & k_{a2} A_{G2} - \frac{CL + CL_{ic}}{V_c} A_c + \frac{CL_{ic}}{V_p} A_p \\ & - \frac{(R_{\max C} - DR_C) k_{v2} \frac{A_c}{V_c}}{K_{vd} + \frac{A_c}{V_c}} + k_{off} DR_C \end{aligned} \quad (\text{A.16a})$$

$$\begin{aligned} \frac{dA_p}{dt} = & CL_{ic} \left(\frac{A_c}{V_c} - \frac{A_p}{V_p} \right) \\ & - \frac{(R_{\max P} - DR_P) k_{v2} \frac{A_p}{V_p}}{K_{vd} + \frac{A_p}{V_p}} + k_{off} DR_P \end{aligned} \quad (\text{A.16b})$$

$$\begin{aligned} \frac{dDR_C}{dt} = & \frac{(R_{\max C} - DR_C) k_{v2} \frac{A_c}{V_c}}{K_{vd} + \frac{A_c}{V_c}} \\ & - (k_{off} + k_{deg}) DR_C \end{aligned} \quad (\text{A.16c})$$

$$\begin{aligned} \frac{dDR_P}{dt} = & \frac{(R_{\max P} - DR_P) k_{v2} \frac{A_p}{V_p}}{K_{vd} + \frac{A_p}{V_p}} \\ & - (k_{off} + k_{deg}) DR_P \end{aligned} \quad (\text{A.16d})$$

Where A_c , A_p [nmol] are the amounts of vildagliptin in the central and peripheral compartments respectively, CL [L min^{-1}] is a non-saturable clearance, CL_{ic} [L min^{-1}] is the inter-compartmental clearance, V_c , V_p [L] are the volumes of the central and peripheral compartments respectively, k_{v2} [min^{-1}] is a parameter added for the slow tight binding of vildagliptin to DPP-4, K_{vd} [nmol L^{-1}] is the equilibrium dissociation constant, k_{off} [min^{-1}] is a rate constant for the dissociation of intact vildagliptin from DPP-4, $R_{\max P}$ [nmol] is the maximum possible amount of DPP-4 in the peripheral compartment, k_{deg} [min^{-1}] is a rate constant for the hydrolysis of vildagliptin by DPP-4, and DR_P [nmol] is the amount of deactivated DPP-4 in the peripheral compartments.

Parameter	Value	Parameter	Value	Parameter	Value
V_{BC}^G [dL]	3.5	V_{BF}^G [dL]	4.5	V_H^G [dL]	13.8
V_L^G [dL]	25.1	V_G^G [dL]	11.2	V_K^G [dL]	6.6
V_{PC}^G [dL]	10.4	V_{PF}^G [dL]	67.4	V_B^I [L]	0.26
V_H^I [L]	0.99	V_G^I [L]	0.94	V_L^I [L]	1.14
V_K^I [L]	0.51	V_{PC}^I [L]	0.74	V_{PF}^I [L]	6.74
V^F [mL]	6.74	Q_B^G [dL min ⁻¹]	5.9	Q_H^G [dL min ⁻¹]	43.7
Q_A^G [dL min ⁻¹]	2.5	Q_L^G [dL min ⁻¹]	12.6	Q_G^G [dL min ⁻¹]	10.1
Q_K^G [dL min ⁻¹]	10.1	Q_P^G [dL min ⁻¹]	15.1	Q_B^I [dL min ⁻¹]	0.45
Q_H^I [L min ⁻¹]	3.12	Q_A^I [L min ⁻¹]	0.18	Q_K^I [L min ⁻¹]	0.72
Q_P^I [L min ⁻¹]	1.05	Q_G^I [L min ⁻¹]	0.72	Q_L^I [L min ⁻¹]	0.9
T_B^G [min]	2.1	T_P^G [min]	5.0	T_P^I [min]	20.0
f_q [·]	0.9	$k_{\phi 1}$ [·]	0.68	$k_{\phi 2}$ [·]	0.00236
k_{12q} [min ⁻¹]	0.08	k_{\min} [min ⁻¹]	0.005	k_{\max} [min ⁻¹]	0.05
k_{abs} [min ⁻¹]	0.08	c_1 [·]	0.067	c_2 [·]	1.59
c_3 [·]	0.62	c_4 [·]	1.72	c_5 [·]	2.03
d_1 [·]	1.126	d_2 [·]	0.683	d_3 [·]	0.14
d_4 [·]	0.023	d_5 [·]	1.59	m_{l_0} [U]	6.33
ζ_1 [L pmol ⁻¹]	0.0026	ζ_2 [L (pmol min) ⁻¹]	0.99e ⁻⁴	K_l [min ⁻¹]	0.3621
K_s [min ⁻¹]	0.0572	γ [$\mu\text{g min}^{-1}$]	2.366	α [min ⁻¹]	0.615
β [min ⁻¹]	0.931	N_1 [min ⁻¹]	0.0499	N_2 [min ⁻¹]	0.00015
V^Ψ [dL]	11.31	K_{out} [min ⁻¹]	68.3041	Cf_2 [min ⁻¹ nmol ⁻¹]	21.1512
τ_ψ [min ⁻¹]	35.1	$R_{\text{max}C}$ [nmol]	5.0	ζ [·]	8.248
f_v [·]	0.772	k_{a1} [min ⁻¹]	0.021	k_{a2} [min ⁻¹]	0.0175
CL [L min ⁻¹]	0.6067	CL_{ic} [L min ⁻¹]	0.6683	V_p [L]	97.3
k_{off} [min ⁻¹]	0.0102	$R_{\text{max}P}$ [nmol]	13	k_{deg} [min ⁻¹]	0.0018
V_c [L]	22.2	K_{vd} [nmol L ⁻¹]	71.9	k_{v2} [min ⁻¹]	0.39
k_{go} [min ⁻¹]	1.88e ⁻⁴	k_{gg} [min ⁻¹]	1.85e ⁻⁴	k_{pg} [min ⁻¹]	4.13
k_{gl} [min ⁻¹]	0.46	k_{pl} [min ⁻¹]	0.00101	k_{lp} [min ⁻¹]	0.91
k_{po} [min ⁻¹]	0.51	$\nu_{GW,\text{max}}$ [·]	0.9720	$\nu_{L,\text{max}}$ [·]	0.7560
$\nu_{P,\text{max}}$ [·]	0.2960	n_{GW} [·]	2.0	n_L [·]	2.0
n_P [·]	5.0	$\phi_{GW,50}$ [·]	431.0	$\phi_{L,50}$ [·]	521.0
$\phi_{P,50}$ [·]	1024.0	ρ_α [min ⁻¹]	54	ρ_β [min ⁻¹]	54
α_M [min ⁻¹]	0.06	β_M [min ⁻¹]	0.1	p_{la} [min ⁻¹]	0.5
r_{la} [·]	0.2143	q_{la} [dL ² mU ⁻²]	3.04e ⁻¹⁰	b_{la} [min ⁻¹]	0.025
C_{max} [·]	15.0	k_{ia} [min ⁻¹]	2.35e ⁻⁵	p_{fa} [min ⁻¹]	0.5
r_{fa} [·]	0.2143	q_{fa} [dL ² mU ⁻²]	1.3e ⁻¹¹	b_{fa} [min ⁻¹]	0.0068
τ_{HR} [min]	5.0	n_e [·]	4.0	a_e [·]	0.8
τ_e [min]	600	α_e [·]	2.974	β_e [bpm ⁻¹]	3.39e ⁻⁴

Table B.1
Parameters Values

B Parameters Mean Values

Table B.1 includes the values of the parameters which were used in the simulation.